Numerical Analysis of a Fuel Pump for an Aircraft Diesel Engine

Rafał Sochaczewski[1*], and *Marcin* Szlachetka[2]

[1] Lublin University of Technology, Faculty of Mechanical Engineering, Nadbystrzycka 36, 20-618 Lublin, Poland
[2] Pope John Paul II State School of Higher Education, Department of Mechanical Engineering, ul. Sidorska 95/97, 21-500 Biala Podlaska, Poland

Abstract. The paper reports on the process of modelling a high-pressure common rail pump designed to supply a two-stroke compression-ignition engine, which includes the presentation of methodology for model construction and results of simulation tests. A one-dimensional model of the pump was developed in the AVL Hydsim environment. A single-section positive displacement pump driven by a double cam was used for modelling. The developed model enables simulation of pump operation in various conditions defined by shaft speed, pumping pressure, settings of pump executive elements as well as fuel properties. The obtained results were compared with the results of bench tests and theoretical calculations. The analysis included the flow rate fuel overflow and changes in pumping pressure depending on the fuel dispenser settings. The model will also be used to build a complete fuel supply system model consisting of an injector model, a rail model and a control system model. The research is carried out with a view to optimising individual components and the operation of the entire supply system, taking into account the regulation of pumping pressure and synchronisation of the pumping process with fuel injection cycles.

1 Introduction

Increasing requirements to reduce exhaust emissions and fuel consumption while not compromising the power factor is currently becoming widely applicable to internal combustion engines intended for aircraft applications. As a result, intensive research works are underway to develop a diesel-powered unit for aircraft propulsion. The paper [1] discusses the parameters of about 40 types of aircraft diesel engines. Due to a number of advantages, such as: lack of the head (lower heat loss) and timing system, opposite movement of pistons conducive to balancing the engine, development and modernisation of the compression-ignition engine operating in a two-stroke cycle and opposing pistons, the design was subjected to development and modernisation [2, 3, 4]. Of course, such a construction also has drawbacks. The main one is the need for the use of a gear connecting two crankshafts or a complicated crank system with one shaft. Due to the specific pistons-sleeves arrangement, it is necessary to place the injector or fuel injectors perpendicularly to the cylinder axis. As a result, it is necessary to develop a new combustion chamber and a power supply system cooperating with this chamber.

In order to facilitate optimisation and limit the number of experiments, numerical modelling analyses are used. Scientific literature describes numerous modelling tests of fuel system elements [5, 6, 7, 8] as well as entire injection systems [9, 10, 11, 12, 13]. By way of illustration, [5] investigated the effect of multiphase injection on the emission of particulate matter and nitrogen oxides, works [6, 7] included micro and macroscopic dynamic phenomena accompanying multiphase injection, whereas [8, 11, 14] – the effect of cavitation on flow loss.

Mathematical modelling is a method often used in the design and testing of aircraft engines. It helps shorten the time from concept to prototype, as in the case with the following models of: the process of combustion [15, 16], cooling systems [1716, 18], charge exchange [19], or whole engines [20, 21].

The paper [22] presents the process of electromagnetic modelling of the common rail injector. The employed computational method optimised the fuel nozzle installed in a commercial injector for use in a two-stroke diesel engine. In order to simulate the operation of the complete fuel system, in the next stage a model of a high-pressure pump was made, which was the primary subject of the work. The model was developed by means of BOOST-Hydsim software tool by AVL– an environment for analysis of fuel supply systems. The module in question is dedicated to dynamic analysis of hydraulic and hydro-mechanical systems and control systems [23, 24, 25, 26]. It is based on the theory of fluid dynamics and vibration of multi-member systems.

This article presents the process of modelling a high-pressure pump for a two-stroke compression-ignition engine and opposing pistons. The engine is at the design stage; the assumed power is 100 kW and capacity 1500 cm^3. The objective of the study is to optimise the pump flow rate in order to supply the engine in all operating conditions, as well as to develop a complete supply system in order to carry out further optimisation works.

* Corresponding author: r.sochaczewski@pollub.pl

2 Materials and methods

2.1 AVL BOOST Hydsim

BOOST Hydsim is a module dedicated to dynamic analysis of hydraulic and hydro-mechanical systems and control systems. It is based on the theory of fluid dynamics and vibration of multi-member systems. Originally, the program was developed to simulate injection systems of compression-ignition engines. At the moment, it enables modelling of petrol, heavy oils and alternative fuels supply systems. In addition, it is supplemented with new applications such as hydraulic transmissions, control of valves and actuators. It can be used to simulate multi-phase injection and systems containing control units.

BOOST Hydsim is an integral tool in the AVL Workspace equipped with a graphical pre-processing editor. The one-dimensional model presented in BOOST Hydsim contains a general image of the system, defined by the user. Models are built from elements grouped depending on their type and functionality. Each specific element of the physical supply system is represented by an icon, a symbol containing a schematic drawing of the element on the GUI (Graphical User Interface). System elements (icons) can be connected with each other by mechanical, hydraulic or logical connections. Thanks to this solution, it is possible to define the supply system in any configuration of component connections. The GUI controls the model building process and prevents connections that do not conform to the input specification.

Input data depends on the configuration of the system and a specific calculation task (*standard calculation*, *restart*, *run with optimisation* or *serial calculations*). A fixed set of input parameters is associated with each element. Some parameters are optional, realised by means of switches. Each element has an identification number and user name. Fluid properties and mechanical connections require separate inputs. In addition, general model calculation control data must be specified.

Each element has a defined set of results, which, after being selected by the user, are stored in ASCII files. Default data and control information are stored in a GIDas file. Its content can be opened directly in *Case Explorer*, which is integrated with *Impress Chart* post-processor. An iteration history file (GAD File) is created to run the optimisation. Two tools are used to present simulation results: *IMPRESS Chart* (allows the user to generate charts using predefined templates or designed by the user) and *PP3* (for flow animations) [15, 16].

2.2 Assumptions of the model

The model was developed in an environment with libraries allowing building a structure of any fuel supply system. The model calculates fuel parameters in particular elements of the fuel pump. This enables visualising simulation results in the form of flow parameters for hydraulic (pressure, temperature, volume or mass flow, geometric and effective flow surface, flow resistance, steam bubbles, cavitation coefficient) and mechanical elements (coordinates, speed, acceleration, dynamic forces and torque, kinematic parameters). Calculation results are available in the time domain or crankshaft rotation angle.

During the construction of the pump model, the following assumptions and simplifications resulting from the specific operation of the program (dimensionality of the mathematical model) were made:

- a one-dimensional model taking into account only the length and diameter of the flow elements,
- the high-pressure pump is a piston displacement pump,
- the pumping sections of the high-pressure pump are geometrically identical,
- the geometric orientation of the elements of the system has no influence on their operation,
- the temperature of the walls of the components is constant,
- fuel flow through pump components includes circular cross-section components,
- the boundary mechanical condition defines a position or velocity in one direction only and is a fixed value,
- elements of the pump are assumed to be non-deformable elements (coordinates and piston velocity between the input and output state are the same),
- volumes are elements with non-deformable walls,
- the volumes were connection by cylinders taking into account the frictional losses determined by the Laplace transform,
- 33 % of the mass of the spring is added to the mass of the moving elements affected by the spring.

2.3 Test object

The CP4 series pump (**Fig. 1**), next version of the Bosch high-pressure pump, was used for the calculation. Compared to the previous generation, the design has been optimised by reducing the number of components and the application of aluminium pump housing. High fuel pressure is generated in the pumping section and is flows directly through high-pressure pipe to the rail - there are no high-pressure fuel channels in the body. It is a single-section positive displacement pump (CP 4.1) driven by a cam roller with a double cam. The pump flow rate is regulated by a dosing valve located in the pump body. The pump has a flange mounting and the possibility of placing a gear wheel on the pump shaft. This makes it possible to install the pump in an engine block and transfer the drive from the gearing. The pump is supplied with fuel by means of a low-pressure electric pump. Pre-pressure is stabilised by means of a bypass valve in the range of 0.45 to 0.5 MPa. The pump is lubricated with fuel. Depending on the number of pumping sections, the drive ratio is 1:1 or 1:2.

Fig. 1. CP4.1 pump.

2.4 Pump model

Based on the geometry of the CP4.1 pump, a pump model was built in the AVL BOOST-Hydsim. A schematic of the pump model is shown in Fig. 2.

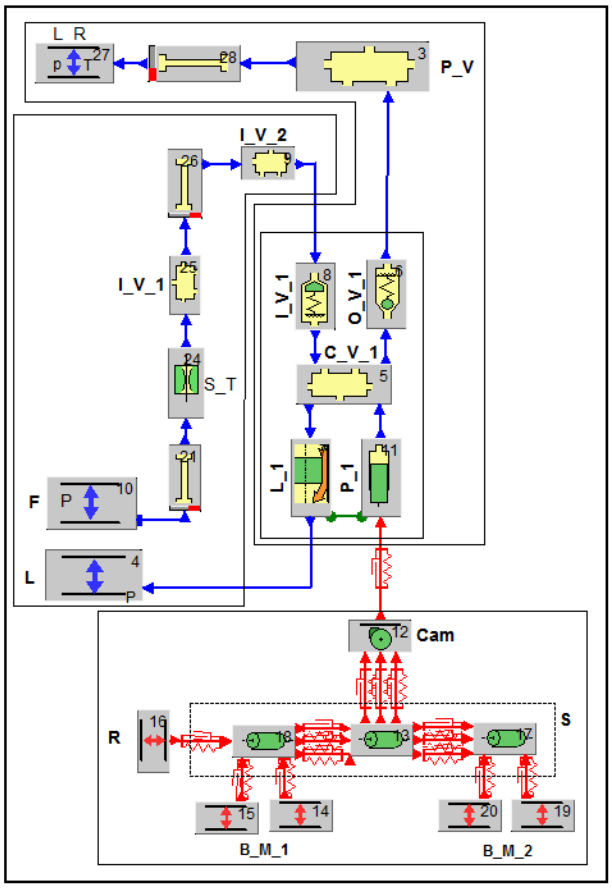

Fig. 2. Scheme of the CP 4.1 pump model.

The high-pressure pump model consists of three blocks. The first block is the pump drive block. This is a shaft double cam roller model. At the bottom of the pump there is a cam drive (*S*) for which the rpm has been defined. The shaft is mounted in the pump casing at two points. The boundary mechanical conditions (*B_M_1* and *B_M_2*) deprived the drive shaft of its degrees of freedom and gave it a rotary motion (*R/16*).

The unit vector of the x-axis of the element in the global coordinate system is determined from the equation:

$$\overrightarrow{X_{lok}} = e_1\overrightarrow{X_{gl}} + e_2\overrightarrow{Y_{gl}} + e_3\overrightarrow{Z_{gl}} \quad (1)$$

where: $\overrightarrow{X_{gl}}, \overrightarrow{Y_{gl}}, \overrightarrow{Z_{gl}}$ are unit vectors in the global coordinate system, e_1, e_2, e_3 are the unit vector components in the global *x*, *y* and *z* direction. Default values for unit vector are 1. / 0. / 0. (global and local coordinate systems are identical).

The cam (*Cam/12*) of the pumping section is located on the drive shaft. The setting window allows the user to define the profile of the cam. The window defines the radius of the basic cam circle, the displacement of the tappet relative to the axis of rotation, the lift and initial speed of the tappet, the angular displacement of the cam relative to the beginning of the calculation. The profile of the cam can be defined by lift or acceleration as a function of shaft rotation.

In the modelled pump, the profile of the cam was defined by introducing lift as a function of shaft rotation. The cam lift was measured (Table 1) and its characteristics were determined (Fig. 3).

Table 1. Pump cam lift values CP4.1.

No	Angle	Lift		No	Angle	Lift
	[deg]	[mm]			[deg]	[mm]
1	0.00	0.000		25	180.00	0.000
2	7.50	0.192		26	187.50	0.207
3	15.00	0.710		27	195.00	0.727
4	22.50	1.460		28	202.50	1.444
5	30.00	2.345		29	210.00	2.356
6	37.50	3.319		30	217.50	3.293
7	45.00	4.191		31	225.00	4.220
8	52.50	5.088		32	232.50	5.115
9	60.00	5.845		33	240.00	5.892
10	67.50	6.520		34	247.50	6.519
11	75.00	7.027		35	255.00	7.030
12	82.50	7.344		36	262.50	7.369
13	90.00	7.433		37	270.00	7.439
14	97.50	7.304		38	277.50	7.300
15	105.00	6.966		39	285.00	6.957
16	112.50	6.399		40	292.50	6.399
17	120.00	5.696		41	300.00	5.680
18	127.50	4.880		42	307.50	4.885
19	135.00	4.006		43	315.00	4.003
20	142.50	2.986		44	322.50	3.108
21	150.00	2.090		45	330.00	2.139
22	157.50	1.236		46	337.50	1.263
23	165.00	0.544		47	345.00	0.547
24	172.50	0.086		48	352.50	0.114

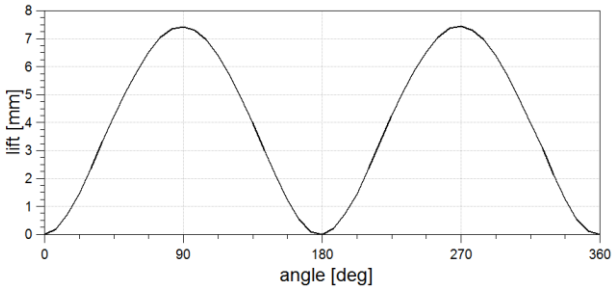

Fig. 3. Profile of the CP4.1 pump drive shaft cam.

The components in the pump drive block are connected by mechanical bonds with a defined connection direction, preload, stiffness and damping.

The second block is a pumping section block which is connected to the pump drive block by means of mechanical bonds (movement of the piston with a displacement caused by rotation of the cam). The pumping section block contains: an axial pump (*P_1/1* - piston with cylinder), volume over piston (*C_V_1/5* - compression chamber) as well as an inlet valve (*I_V_1/8)* and an outlet valve (*0_V_1/6*). The pumping section is non-deformable and is defined by the mass in progressive motion, piston diameter, friction force, pressure in the

piston chamber and spring parameters in the pumping section.

The pumping section is connected by a hydraulic line with a compression chamber of a preset volume to which a ring gap (*L_1/7*) is connected. The function of this element is to model fuel leaks between the cooperating elements of the pumping section. For this reason, the leakage is connected to the pump (element *P_1/1*) by a special functional connection. This means that both elements are parts of a certain physical unit. Each leak is defined by the initial fixed leakage length and the gap between the piston and cylinder as a function of pressure.

Fuel from the pumping section is channelled through a (*P_V/3*) channel located in the pumping section to the stub pipe connecting the pump with the rail.

The leakage model is based on the Hagen-Poiseuille law. It considers steady laminar flow through annular gap because small cross-sectional gap area results in laminar flow. As fluid enters the annular gap, the velocity profile is linear. The fluid velocity at the barrel wall is equal to barrel velocity and at the piston wall is equal to piston velocity. This layer of fluid exerts considerable shear forces on the inner layers whose velocities must exceed the piston velocity v_p to satisfy the law of continuity. In the case of constant laminar flow through the ring gap, the Navier-Stokes equation takes the form of:

$$\frac{dp}{dx} = \mu \frac{d^2v}{dy^2} \tag{2}$$

where: x, y – coordinates of motion, v – fluid velocity in x direction, p – pressure μ – dynamic viscosity.

Flow rate through leakage gap is defined by:

$$\dot{Q} = \frac{\pi}{\mu}\frac{p_{out}-p_{in}}{L_{gap}}\left[\frac{1}{4}\left(R_b^4 - R_p^4\right) - \frac{1}{3}\left(R_b + R_p\right)\left(R_b^3 - R_p^3\right) + \frac{1}{2}R_b R_p\left(R_b^2 - R_p^2\right)\right] + \\ + \pi\left(v_b - v_p\right)\left[\frac{2}{3}\frac{R_b^3 - R_p^3}{R_b - R_p} - R_p\left(R_b + R_p\right)\right] + \pi v_b\left(R_b^2 - R_p^2\right). \tag{3}$$

where: p_{in}. p_{out} – pressure on input/output side of piston, L_{gap} – gap length, R_b. R_p – radius of barrel/piston, v_b. v_p – velocity of barrel/piston.

Inlet and outlet valves are defined by: masses in progressive motion, maximum lift, coefficient of flow resistance through the valve at the largest opening of the valve, pressure differences for valve opening. Parameters of valve seat and valve spring were also determined. in the adopted linear model of a valve in the seat stiffness and damping are constant, and at positive distances there is no clamping force.

The motion of the valve masses in the local coordinate system is given by the equation:

$$m\ddot{x} + c_0\dot{x} + k_0 x = -F_0 - F_{hyd} - F_{damp} - F_{in_{st}} - F_{out_{st}} \tag{4}$$

where: m – valve mass, x – valve coordinate, c_0. k_0 – damping and stiffness constants of the valve spring, F_0 – preload force of the valve spring, F_{hyd} – hydraulic force, F_{damp} – damping force of squeezing fluid at valve closing, F_{in_st}. F_{out_st} – additional forces from input and output stops.

The third block is the part of the pump responsible for supplying fuel to the pumping section and removing fuel from the pump. Fuel for pumping sections is delivered from a low pressure system defined by boundary conditions F/10 by determining temperature and pressure of medium as a function of time (optional rotation angle). Fuel flows through line (/21) to a flow control orifice (*S_T/24* - orifice simulates the operation of the dispenser of fuel) and then the volume *I_V_1/25* and *I_V_2/9* goes to the pumping section. Excess fuel from the pump is directed to the low-pressure part of the system specified by *L* conditions.

Hydraulic boundary conditions were assumed for the calculations: *F/10* corresponds to the parameters of fuel supplied to the pumping sections: pressure 0.3 MPa and temperature 313 K; *L* - overflow of fuel: pressure 0.1 MPa and temperature 313 K; *L_R* - fuel pumped to the rail: pressure from 30 to 140 MPa, temperature 323 K. The fuel used is diesel oil with a density of 850 kg/m^3 and temperature and pressure corresponding to boundary conditions.

3 Results

This section presents the results from simulation studies. In the first stage the numerical results were compared with available results obtained from bench tests. Fig. 4 presents a comparison of pump output obtained from model (Hydsim), bench tests and theoretical calculations – based on the size of the pumping section. The pump output obtained from model tests was the sum of volumetric flow rate of fuel from the pumping section and fuel from section leaks. It was assumed that the fuel dispenser is fully open and the rotational speed of the pump shaft changed. The pumping pressure was assumed to be 30 MPa. The most significant differences in flow rates are for the pump shaft speed of 2500 rpm, which amounts to approx. 2.5 %. As the speed decreases, the difference decreases to about 1.5 %.

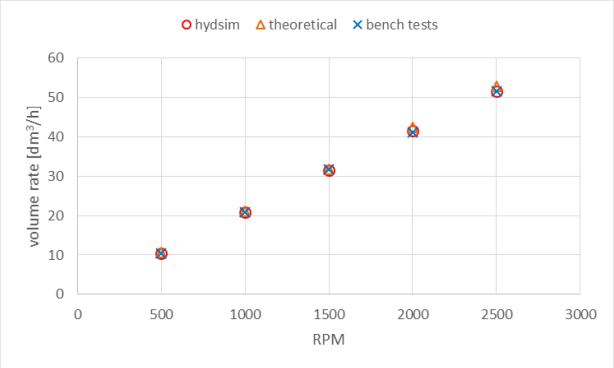

Fig. 4. Flow rate characteristics of CP4.1 pump (Hydsim, theoretical and bench tests).

Fig. 5 shows a comparison of the pumping pressure during one rotation of the pump shaft. The pressure waveforms exhibit slight differences, which may be attributed to the fact that in the model the preset pressure in the reservoir was regulated by means of a check valve, while in the case of bench tests - by means of a bleed valve controlled by the PID regulator. However, the pressure ranges are comparable.

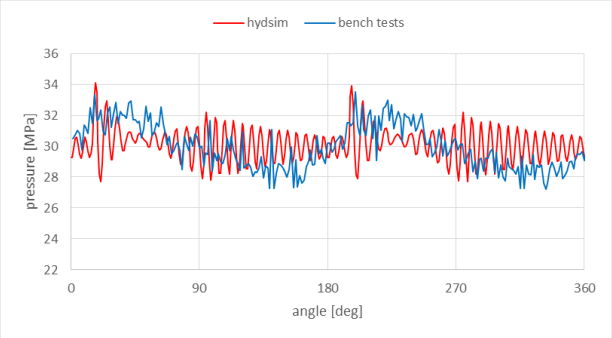

Fig. 5. Pressure waveform (Hydsim, bench tests).

For the same operating conditions, the torque waveform and amplitude on the pump shaft (Fig. 6) were compared.

Fig. 6. Torque waveform (Hydsim, bench tests).

In the next stage, tests simulating the operation of the dosing device regulating the amount of incoming fuel to the pumping section were carried out. The function of the dispenser is performed by an orifice (*S_T/24*) with adjustable flow cross-sectional area. The flow field changed from 0.25 mm^2 to 1.00 mm^2 at 0.25 mm^2 steps. As the flow area field decreases, the flow rate (Fig. 7) and the amount of leakage through the pumping section (Fig. 8) decreases. The pumping rate decreases by approx. 32%. and leaks by approx. 20%.

Flow throttling causes the pumping section to become filled only partially. Fig. 9 shows the pressure in the pumping section chamber. There is a delay in pumping due to throttling the flow of fuel flowing into the pumping section and as a result the piston stroke is reduced and the shaft contact with the pusher is delayed.

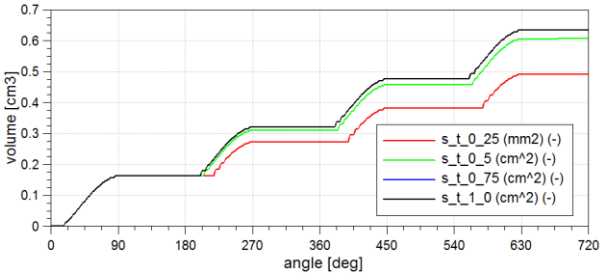

Fig. 7. Volume of fuel flowing out of the pumping section depending on the orifice size.

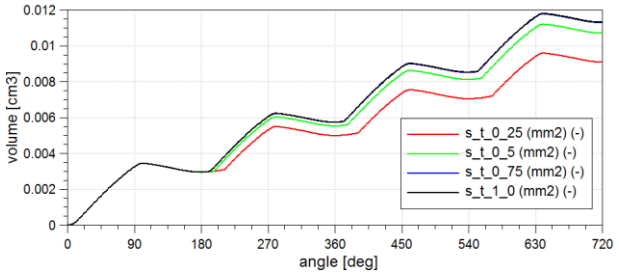

Fig. 8. Volume of fuel flowing through the leakage depending on the orifice size.

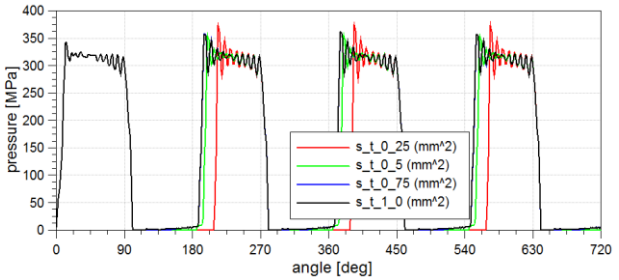

Fig. 9. Pressure waveforms in the pumping section chamber C_V_1/5.

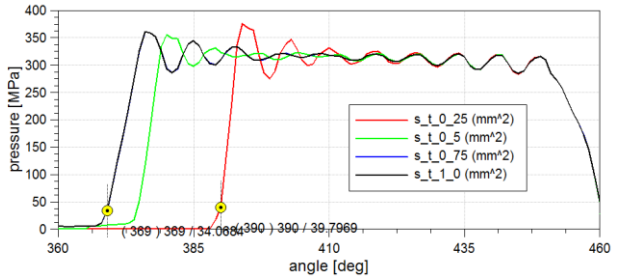

Fig. 10. Pressure waveforms in the discharge section chamber C_V_1/5 on a narrow scale.

Fig. 10 shows the changes in a narrow scale of the rotation angle of the pump drive shaft. The differences in the discharge delay are maximum 20% for a flow area from 0.25 to 0.75 mm^2, whereas above 0.75 mm^2 no differences in the pressure curve were observed, which means that the volume of the delivery section is completely filled with fuel.

4 Conclusions

The developed numerical model of the common rail high-pressure pump gives relatively good results, comparable with bench tests and theoretical calculations. The model will be used for optimisation tests of the pump and cognitive dynamic, cavitation, *etc.* phenomena occurring during the flow of liquid through the pump elements, especially at high pressures.

The model will furthermore be applied in the construction of the entire power supply system for a two-stroke diesel engine with opposing pistons. The research will optimise the work of the injector as well as the control algorithm in terms of pressure regulation and synchronisation of the pumping process with fuel injection cycles.

In relation to the obtained simulation results, the model needs certain modifications. This will require additional experimental tests and calibration of the model.

This work has been realised in cooperation with the Construction Office of WSK "PZL-KALISZ" S.A." and is part of Grant Agreement No. POIR.01.02.00-00-0002/15 financed by the Polish National Centre for Research and Development.

References

1. M. Gęca Michał, Z. Czyż, M. Sułek, Combustion Engines, **169** (2017)
2. J. Pirault, M. Flint, SAE (2009)
3. J. Heywood, (1988)
4. M. Franke, H. Huang, J. Liu, SAE (2006)
5. V. Amoia, A. Ficarella, D. Laforgia, S. De Matthaeis, SAE (1997)
6. G. Bianchi, P. Pelloni, F. Corcione, F. Luppino, SAE (2001)
7. L. Catalano, V. Tondolo, A. Dadone, SAE (2002)
8. A. Ficarella, D. Laforgia, V. Landriscina, SAE (1999)
9. C. Gautier, O. Sename, L. Dugard, G. Meissonnier, IFAC (2005)
10. P. Lino, B. Maione, A. Pizzo, Appl Math Model (2007)
11. R. Payri, H. Climent, F. Salvador, P I Mech Eng D-J AUT (2004)
12. X. Seykens, L. Somers, R. Baer, MECCA (2005)
13. X. Seykens, L. Somers, R. Baer, VAFSEP (2004)
14. C. Arcoumanis, M. Gavaises, E. Abdul-Wahab, V. Moser, SAE (1999)
15. Z. Czyż, K. Pietrykowski, Adv. Sci. Technol. Res. J., **8** (2014)
16. A. Nazarewicz, K. Pietrykowski, M. Wendeker, J. Czarnigowski, P. Jakliński, M. Gęca, PTNSS CONGRESS, **SC2** (2007)
17. K. Pietrykowski, T. Tulwin, SAE, **8** (2015)
18. Ł. Grabowski, Z. Czyż, K. Kruszczyński, SAE 2014-01-2883 (2014)
19. Ł. Grabowski, K. Pietrykowski, P. Karpiński, ITM WEB OF CONFERENCES, **15** (2017)
20. Z. Czyż, Ł. Grabowski, K. Pietrykowski, J. Czarnigowski, M. Porzak, Measurement, **113** (2018)
21. P. Magryta, K. Pietrykowski, M. Gęca, Transactions of the Institute of Aviation, **250** (2018)
22. R. Sochaczewski, Z. Czyż, K. Siadkowska, Combustion Engines **170** (2017)
23. AVL BOOST Hydsim Primer, (2013)
24. AVL BOOST Hydsim User Guide (2013)
25. V. Caika, P. Sampl, SAE (2011)
26. A. Pirooz, Indian J.Sci.Res., **5** (2014)